Striped and Spotted Pattern Generation on Reaction-diffusion Cellular Automata – Theory and LSI Implementation –

Youhei Suzuki[1], Takahiro Takayama[2] Ikuko N. Motoike[2], and Tetsuya Asai[1]

[1] Graduate School of Information Science and Technology, Hokkaido University, Kita 14, Nishi 9, Kita-ku, Sapporo, 060-0814 Japan
[2] Future University - Hakodate, 116-2 Kamedanakano-cho Hakodate Hokkaido, 041-8655 Japan

Abstract. A novel reaction-diffusion cellular-automaton model that generates Turing-like spatial patterns is proposed. The model employs linear diffusion fields of activators and inhibitors and a discrete transition rule after diffusion. Theoretical analysis of the one dimensional model proved that i) spatial distribution given by a periodic square function is stable at the equilibrium and ii) the spatial frequency is inversely proportional to the square root of a diffusion coefficient of the inhibitors. We also designed LSI circuits that implement the RD model on a silicon chip that has a compact construction and low-power consumption. Circuit simulations revealed that the proposed LSIs could restore stripe and spot images in a short time regardless of the number of pixels in the image.

1 Introduction

In the process of ontogeny in a multicellular organism, the organism develops from a fertilized egg into matured differentiated cell groups, through repeated division/differentiates. Turing [1] suggested the concept of "Diffusion (driven) instability" for phenomena in systems where diffusion is able to enhance transition from a homogeneous state to a spatially in-homogeneous stable state. In his framework, time development in the system is described by the sum of reaction and diffusion. The former represents local production/extinction of the substance or state and the latter represents a transport process, which tends to dampen any inhomogeneity of the neighboring region, called the reaction-diffusion (RD) system. He gave an example where the spatial instability of a spatial homogeneous structure could take place through the addition of the diffusion effect. This Turing RD model is well known as one in which stable striped or spotted patterns are generated.

There are many ordered complex patterns in nature. For example, we can see patterns in animal skins where the patterns are formed spontaneously. Turing's and modified RD models have been studied because of their significance in explaining pattern formations on animal skins. Striped patterns can not only be seen in animal skin but also human fingerprints. Fingerprint patterns give

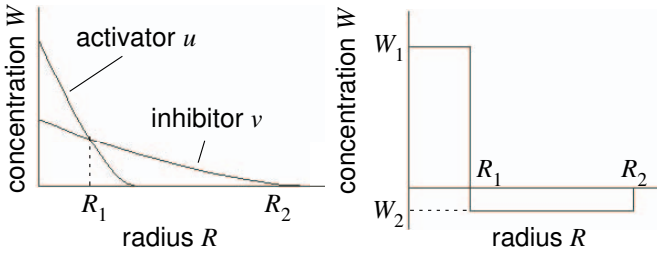

(a) (b)

Fig. 1. Diffusion of activators and inhibitors on (a) continuous model and (b) discrete model.

us important cues for distinguishing individuals. Recent progress with digital microprocessors will certainly push advances in intelligent security systems that recognize fingerprints patterns. This paper deals with the basic mechanism and implementation of restoring striped/spotted patterns. We utilized spontaneous pattern formation with the RD Turing model to design the hardware RD system on a silicon chip that had compact and low-power construction.

2 Model and the Theoretical Analysis

We propose the use of RD systems as models for generating marking patterns on animals. The RD system is a complex system in which the reaction and diffusion of chemical species coexist under nonequilibrium conditions. It produces a variety of orders, rhythms, and self-organizing phenomena observed in nature and in life. Typical examples of such patterns are marking patterns on various animals, which are referred to as Turing patterns [2, 3].

Turing patterns can usually be obtained by solving mathematical RD models described by a set of partial differential equations (PDE) that are represented by continuous spatiotemporal variables. Several attempts to reproduce Turing patterns with limited computational resources have been made over the years [4–9]. A typical example is the use of cellular automata (CA) where the space is separated by a set of discrete cells, and time and cell state are represented by discrete values. Gerhardt, Schuster and Tyson have discretized the RD model based on chemical system [5, 6]; Markus and colleagues have shown the way to avoid unisotropy of the pattern and described various shell patterns [7]; Weimar, Tyson, and Watson have generalized CA model based on RD model and evaluated CA in relation to PDE [8, 9]. In the way to construct CA model, simplifying the nonlinear dynamics in a continuous RD model is a difficult task because the differential equations are rewritten by conditional divergence rules in the CA.

Young [4] proposed a simplified discrete CA model for describing Turing patterns. He introduced a discrete model for diffusion effects between chemical

substances and represented all the states (usually they had two variables; i.e., activators and inhibitors) with a single binary {1,0} variable. Then, he further simplified the diffusion of the two chemical substances.

One necessary condition for generating Turing patterns is that activators only influence their local neighbors (hard to diffuse), while inhibitors not only influence their neighbors but distant cells (easy to diffuse). Figure 1(a) illustrates the diffusion profile of activators and inhibitors in a continuous model, where R represent the distance from the center of diffusion, R_1 the position where activators and inhibitors have the same concentration, and R_2 the position where the concentration of inhibitors is asymptotically zero. When $R < R_1$, activators and inhibitors produce "active effects" on the field because the concentration of activators is higher than that of inhibitors. When $R_1 < R < R_2$, they produce "inhibitory effects" because the concentration of inhibitors is higher.

Young simplified the effects on distance R as we illustrated in Fig. 1(b). In his CA model, a cell whose state is "1" within $R < R_1$ has positive effects W_1, while a cell whose state is "1" within $R_1 < R < R_2$ has negative effects W_2. The transition of a cell in position $\mathbf{r}$ is determined by the weighted-sum of cells within $R < R_2$ whose states are "1" expressed as $\sum_{|\mathbf{r}-\mathbf{r_i}|\leq R_2} W$, where W represents the weight strength. If the summed value is zero, no transition occurs, while if the value is positive (or negative), the subsequent state of the cell is set to "1" (or "0"). This *step* transition rule corresponds to chemical reactions in continuous RD models. Young showed that stripe patterns and then spot patterns appeared on the CA with fixed R_1, R_2 and W_1 by changing the value of W_2. Surprisingly, all the patterns became stable within 10 steps, even when random initial patterns were given to the CA.

2.1 A modified RD CA model

In Young's simplified CA, the diffusion terms in the continuous RD model are represented by the weighted summation of neighboring cells, while the reaction terms in the RD model are represented by the sign of the sum. Therefore, to describe a cell's transition, the cell has to refer to its neighboring cell's states. Since the number of neighboring cells is approximately calculated by $\pi \times R_2 \times R_2$, the number of physical connection wires (on CA hardware) to refer the neighboring cell's states increases significantly when R_2 increases. Moreover, the CA cannot generate spatially smooth patterns because step functions are used in the cell transition rule. A promising solution to these problems is using a discrete diffusion equation with a four-point spatial approximation method and an analog sigmoid function in the rule instead of the step function. Based on Young's simplification, we propose a novel RD CA model that is suitable for LSI implementation where a cell's transition is determined by the sigmoid function and weighted-summing computation is only restricted within the cell's nearest neighbors.

The weighted-summing computation described above is done by the diffusion fields. In other words, activators and inhibitors diffuse in individual diffusion fields and are then convoluted by a 2D array of cells. Each cell's state

is determined by the difference between the concentration of activators, u, and inhibitors, v, at a given spatial point, (x, y). Diffusion equations for variables u and v are integrated for time δt. Then a cell's subsequent state is determined by the value of the sigmoid function for $u - v$. The dynamics can be formulated as

1. (Diffusion)
   $\partial u(\mathbf{r}, t)/\partial t = D_u \nabla^2 u(\mathbf{r}, t)$,
   $\partial v(\mathbf{r}, t)/\partial t = D_v \nabla^2 v(\mathbf{r}, t)$,
2. (Reaction)
   $u(\mathbf{r}, \delta t(n+1)) = v(\mathbf{r}, \delta t(n+1)) = f\big(u(\mathbf{r}, \delta t \cdot n) - v(\mathbf{r}, \delta t \cdot n) - c\big)$,
   $f(x) = \big(1 + \exp(-\beta x)\big)^{-1}$,

where n represents the time step, $\mathbf{r} = (x, y)$, c is the offset value of the sigmoid function, and β is the slope of the function. We defined this sequential operation as "one cycle". In the following, we show that the system produces spatiotemporal patterns by repeating this cycle.

2.2 Theoretical Analysis

We analyze operations for the proposed model in 1D space and reveal the relation between the spatial frequency of equilibrium patterns and diffusion coefficients.

Since an impulse response of a diffusion equation is represented by the Gaussian, that of $u - v$ is given by a 'difference of Gaussian' (DoG) function:

$$\mathrm{DoG}(x, t) = \frac{1}{\sqrt{4\pi t}} \left[\frac{1}{\sqrt{D_u}} \exp\left(\frac{-x^2}{4 D_u t} \right) - \frac{1}{\sqrt{D_v}} \exp\left(\frac{-x^2}{4 D_v t} \right) \right], \tag{1}$$

where x represents the space. Differential distribution $u - v$, after activators and inhibitors are diffused for time δt, is thus given by

$$z_n(x) \equiv \int_{-\infty}^{\infty} r_n(x - X) \cdot \mathrm{DoG}(X, \delta t)\ dX, \tag{2}$$

where $r_n(x)$ represents an initial input to u and v at the n-th cycle. Therefore, the dynamics of the proposed model can be represented by

$$r_{n+1}(x) = f[z_n(x)], \tag{3}$$

where $r_{n+1}(x)$ represents the subsequent initial input. Assuming the equilibrium state, we obtain

$$r^*(x) = f[z^*(x)], \quad z^*(x) = \int_{-\infty}^{\infty} r^*(x - X) \cdot \mathrm{DoG}(X, \delta t)\ dX, \tag{4}$$

where $z^*(x)$ and $r^*(x)$ represent the equilibrium distribution of $u - v$ and the resulting sigmoid outputs. Assume the equilibrium distribution is

$$r^*(x) = \begin{cases} 1\ (-a < x < a) \\ 0\ (\text{else}), \end{cases} \tag{5}$$

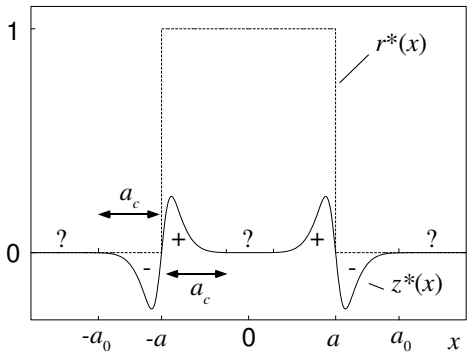

Fig. 2. DoG responses of proposed model for single square-pulse input.

where $a > 0$. For this input, we obtain

$$z^*(x) = \int_{x-a}^{x+a} \mathrm{DoG}(X, \delta t)\, dX, \tag{6}$$

$$= \frac{1}{2}\left[\mathrm{erf}\left(\frac{x+a}{p_u}\right) - \mathrm{erf}\left(\frac{x-a}{p_u}\right) - \mathrm{erf}\left(\frac{x+a}{p_v}\right) + \mathrm{erf}\left(\frac{x-a}{p_v}\right)\right], \tag{7}$$

where $p_{u,v} \equiv \sqrt{4D_{u,v}\delta t}$ and $\mathrm{erf}(\cdot)$ represents the error function. To ensure that input $r^*(x)$ is stable, $z^*(x)$ must be positive for $-a < x < a$, and be negative for other x. Figure 2 plots function $z^*(x)$ for given $r^*(x)$ when $D_u = 0.01$, $D_v = 0.1$, $\delta t = 0.01$, and $a = 0.2$. In this example, we see that the sign of $z^*(x)$ for the center ($x \approx 0$) and surrounds ($|x| > a_0$ in the figure) is indefinite because of $z^*(x) \approx 0$ in these regions. This results in unstable $r^*(x)$ at $x \approx 0$ and $|x| > a_0$.

An error function can be represented in the form of a normal (Gaussian) distribution

$$\frac{\mathrm{erf}(x)}{2} = \int_0^{\sqrt{2}\sigma x} \frac{1}{\sqrt{2\pi}\sigma} \exp\Big(-\frac{y^2}{2\sigma^2}\Big) dy, \tag{8}$$

where σ^2 represents the variance. Using the 3σ law of the Gaussian, we can approximately obtain the values of x where $z^*(x) \approx 0$ as

$$x = -a - \frac{3p_v}{\sqrt{2}},\ -a + \frac{3p_v}{\sqrt{2}},\ a - \frac{3p_v}{\sqrt{2}},\ \text{and}\ a + \frac{3p_v}{\sqrt{2}}, \tag{9}$$

which indicates that the region $-2a \le x \le 2a$ of $r^*(x)$ is stable as long as $a \le 3p_v/\sqrt{2}$ ($\equiv a_c$). Therefore, for a periodic square-wave input,

$$r^*(x) = \begin{cases} 1 \ \Big((4n-1)a < x < (4n+1)a\Big), & (n = 0, \pm 1, \pm 2, \ldots) \\ 0 \ (\text{else}), \end{cases} \tag{10}$$

whose primary spatial frequency f_0 is given by $1/4a$, we conclude that a square wave of $f_0 \ge 1/4a_c = \sqrt{2}/12p_v$ is stable in the subsequent cycle.

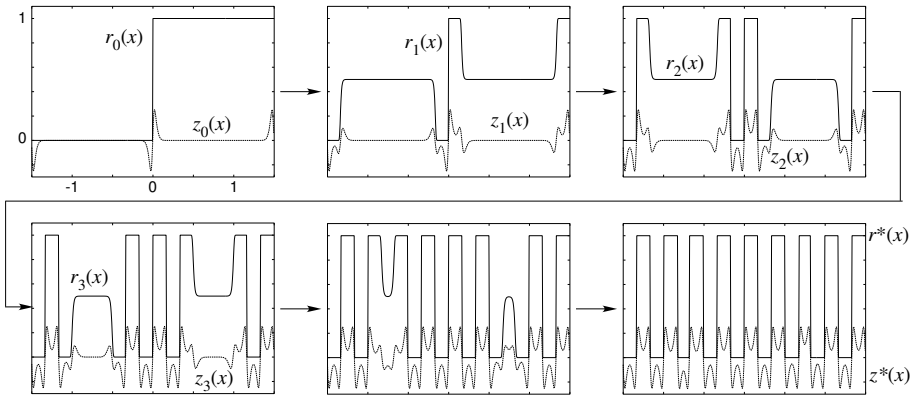

Fig. 3. Pattern formation on 1D model.

For periodic waves of $f_0 < 1/4a_c$, regions of x where $z^*(x) \approx 0$ will exist, which results in $r^*(x) \approx 0.5$ (not 0 or 1). We estimate this region by employing piecewise linear function $f_{\mathrm{pwl}}(\cdot)$ instead of sigmoid function $f(\cdot)$. Because $df/dx|_{x=0} = \beta/4$, we obtain

$$f(x) \approx f_{\mathrm{pwl}}(x) \equiv \begin{cases} \beta x/4 + 0.5 \ (-2/\beta \leq x \leq 2/\beta) \\ 1 \ (x > 2/\beta) \\ 0 \ (x < -2/\beta), \end{cases} \tag{11}$$

which means that $r^*(x)$ will not take 0 or 1 when $-2/\beta \leq z^*(x) \leq 2/\beta$. Therefore, the value of x where $z^*(x) = \pm 2/\beta$ determines stable wave frequency. To calculate this, we considered the following $z^*(x)$,

$$z^*(x) = \frac{1}{2}\left[\mathrm{erf}\left(\frac{x+a}{p_u}\right) - \mathrm{erf}\left(\frac{x+a}{p_v}\right)\right], \tag{12}$$

around $x = -a$ for simplicity. When the argument of the error function is large, the following asymptotic expansion can be used:

$$\mathrm{erf}(x) \approx 1 - \frac{1}{x\sqrt{\pi}} \exp(-x^2). \tag{13}$$

Therefore, when $p_u \ll p_v$ ($d_u \ll d_v$), one has

$$z^*(x) \approx \frac{1}{2\sqrt{\pi}}\left[\frac{p_v}{x+a} \exp\left(-\frac{(x+a)^2}{p_v^2}\right)\right]. \tag{14}$$

The value of x where $z^*(x_0) = 2/\beta$ is thus given by

$$x_0 = p_v\sqrt{\frac{F(2/k^2)}{2}} - a, \tag{15}$$

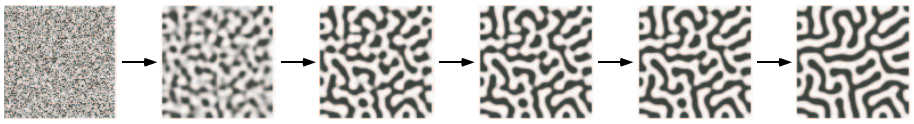

Fig. 4. Snapshots of stripe-pattern formation observed with our proposed model.

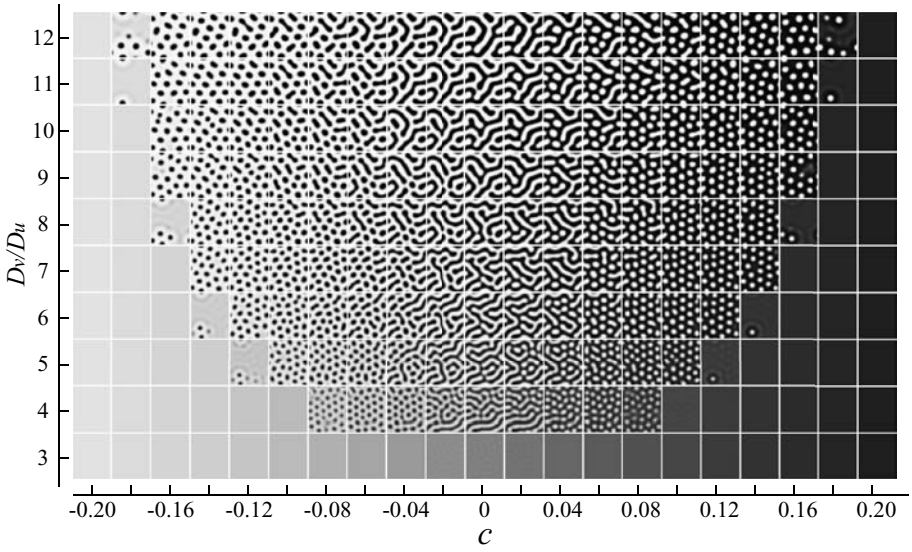

Fig. 5. Pattern diagram for proposed RD model.

where $k \equiv 4\sqrt{\pi}/\beta$ and $F(\cdot)$ represents the inverse function of Lambert's W function. Therefore, we can conclude that i) $r^*(x)$ is not stable when the wavelength is larger than $2x_0$ and ii) the stable wavelength is proportional to p_v (square root of D_v).

Figure 3 has the simulation results for $\delta t = 0.01, D_u = 0.01, D_v = 0.1$ and $\beta = 10^4$ with a cyclic boundary condition. Step input was given at the initial cycle. After a few iterations, a stable square wave appeared. The primary spatial-frequency agreed well with the theoretical prediction ($f_0 = 0.5x_0$). Furthermore, by changing the values of D_v, we numerically confirmed that the equilibrium wave frequency is inversely proportional to the square root of D_v.

Figure 4 is an example of striped pattern formation on a 2D model ($D_v/D_u = \beta = 10$, $c = 0$, $\delta t = 1$). The values of $f\big(u(\mathbf{r}, \delta t \cdot n) - v(\mathbf{r}, \delta t \cdot n) - c\big)$ are represented on a grayscale ($f(\cdot) = 0$: black, $f(\cdot) = 1$: white). The initial state was randomly set within the values of [0:1]. After approximately 10-cycle updates, a stable striped pattern was generated. The space was filled with striped patterns according to the initial spatial distribution. Therefore, if a striped pattern such as a fingerprint pattern is given to the CA, local patterns that do not fit the

striped global patterns are replaced with striped patterns based on the global patterns.

Figure 5 shows a pattern diagram for two variable parameters (D_v/D_u and c). When the value of c was increased, the resulting patterns changed from black spotted to white spotted via the stripe patterns. Also, the spatial frequency could be controlled by the value of D_v/D_u. That is, we can control the form of target patterns (spotted or striped) and the spatial resolution with these two parameters.

Physically, parameter c represents a total balance of activators u and inhibitors v in the model. When $c > 0$, v is predominant over u because the values of u must be larger than that of $v+c$ to ensure $f(u-v-c) > 0.5$, and vice versa when $c < 0$. This can easily be confirmed from Fig. 5 where the area occupied by inhibitors (black areas) is equal to the area occupied by activators (white) when $c = 0$, while inhibitors (black areas) become predominant as c increases.

3 RD Chip Architecture

We designed an RD chip for the RD model described in the preceding section. The basic concept was the use of a CA structure where i) each cell circuit had state memories and a diffusion circuit, and the differential amplifier had a sigmoidal response function, and ii) each cell was only connected to nearest-neighbor cell circuits to reduce the complexity of wiring.

Figure 6 illustrates the unit cell circuit we propose. It consists of a main memory circuit for the state variable (C_{m1} and C_{m2} with master-slave memory structure), a temporal memory (C_{ma}), a diffusion circuit with floating gates (FGs), a differential amplifier that has a sigmoidal response function (DIF), three buffering circuits (voltage followers labeled VF1-VF3), and five transfer gates.

Let us first describe the operations of the diffusion circuit. Let V_{c} and V_{fg} denote the voltage stored in a cell's main memory and that of the FG, respectively. If the initial charge, Q_0, of the FG is zero and the input gate capacitance of VF1 (C_{ox}) is much smaller than the capacitance of control gates C, then V_{fg} is given by

$$V_{\mathrm{fg}} = \frac{V_{\mathrm{n}} + V_{\mathrm{w}} + V_{\mathrm{s}} + V_{\mathrm{e}} + 4\ V_{\mathrm{c}}}{8}, \tag{16}$$

where V_{n}, V_{w}, V_{s}, and V_{e} represent the voltages stored in a neighboring cell's main memory. Assuming that each cell can store V_{fg} in a memory circuit, we obtain

$$\frac{V(t+\Delta t) - V(t)}{\Delta t} = \frac{V_{\mathrm{n}} + V_{\mathrm{w}} + V_{\mathrm{s}} + V_{\mathrm{e}} - 4\ V(t)}{8\Delta t}, \tag{17}$$

where $V_{\mathrm{fg}} = V(t+\Delta t)$ and $V_{\mathrm{c}} = V(t)$. This equation corresponds to the diffusion equation

$$\partial V(\mathbf{r}, t)/\partial t = D\nabla^2 V(\mathbf{r}, t), \tag{18}$$

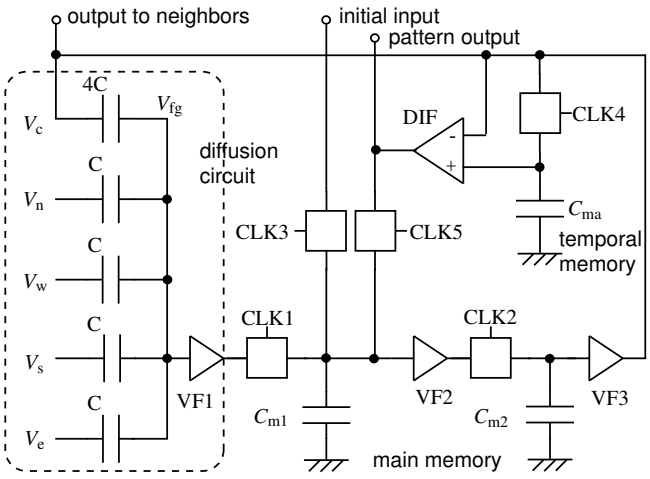

Fig. 6. Construction of unit cell circuit.

when the discrete space is represented on a square grid ($h \equiv \Delta x = \Delta y$ and $D = h^2/(8\Delta t)$). Therefore, by storing $V_{\rm fg}$ in memory and updating this repeatedly, the circuit can solve the discrete diffusion equation. The circuit employed a master-slave analog memory for safe memory updates where the master and slave operations were controlled by CLK1 and CLK2.

Our RD model, as it stands, requires two diffusion fields for variables u and v. Therefore, we propose a novel circuit architecture that has the same operation as our model using only *one* diffusion circuit. The diffusion coefficient and time are always represented in the solution to diffusion equations in the form of $D \cdot t$, which indicates that diffusion and time are interchangeable. For example, let us assume $D_v/D_u \equiv \Delta t_0/\Delta t_1$, and after diffusion for Δt_0 in one diffusion field, the diffused state is stored in a temporal memory, ($C_{\rm ma}$). The memorized voltage is further diffused for $\Delta t_1 - \Delta t_0$. At this time, the voltage in the main memory is equivalent to the voltage after diffusion with D_v for Δt_0. Since temporal memory $C_{\rm ma}$ stores the voltage after diffusion with D_u for Δt_0, one can obtain a diffused distribution for Δt_0 with different diffusion coefficients D_u and D_u, with one diffusion circuit and a temporal memory.

After one-cycle diffusion for Δt_0, the voltage stored in the main and temporal memories is supplied to the differential amplifier (DIF), which has a sigmoid transfer function. By employing FG MOSFETs in the differential pair, we can control offset value c for the sigmoid function. It should be noted that parameter β in the sigmoid function determines the smoothness of generated patterns. If $\beta \to \infty$, the function becomes a step function, which implies that the resulting patterns will not be smooth. The value of β is determined by the rate of FG capacitances for input and control gates, and cannot be controlled after the chip has been fabricated. The output of DIF is stored in $C_{\rm m1}$ by CLK5 evoked in the subsequent step. CLK3 is a control clock that captures an initial voltage, which

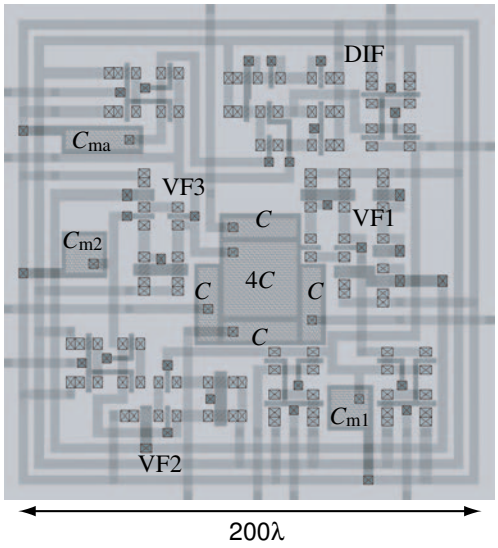

Fig. 7. Layout pattern of unit cell with fixed c (=0) for fingerprint restoration.

is produced by the photodiode or electrostatic sensors mounted on each cell, in the main memory circuit.

The cell circuit was designed by assuming a standard n-well double-poly double-metal CMOS process for fabrication. Figure 7 shows the layout (λ represents the scaling parameter).

4 Simulation Results

We simulated the operations of a 2D array for the proposed cell circuit (180×180 cells). The circuit parameters were $C = 100$ fF, $C_{ox} = 1$ fF, $C_{m1} = C_{m2} = C_{ma} = 100$ fF, and $D_v/D_u = 10$. One cycle in the simulation was performed in 80 steps (8 steps for diffusion with D_u and 72 steps for D_v). The chip required 2 clocks for one-step operation because of master-slave memory operation.

Figure 8(a) has snapshots of pattern formation in the circuit. We could estimate that the system produces striped patterns when $c = 0$ from Fig. 5. Therefore, we used a fingerprint pattern as an initial input. We confirmed that noisy local patterns were repaired by their surrounding striped patterns, as time increased. The circuit required 50 cycles (8000 clocks) to reach equilibrium. Figure 8(b) shows the results for $c = 0.16$ (offset voltage of DIF was set at $0.16 \times V_{dd}$). The same initial input as in Fig. 8(a) was given to the circuit. As expected from Fig. 5, spotted patterns were obtained. The pattern formation process was the same as in Fig. 8(a) where noisy local spots were restored by surrounding global spotted patterns. Therefore, this circuit would be suitable for restoring regularly-arranged spotted patterns such as polka-dot patterns. The system took

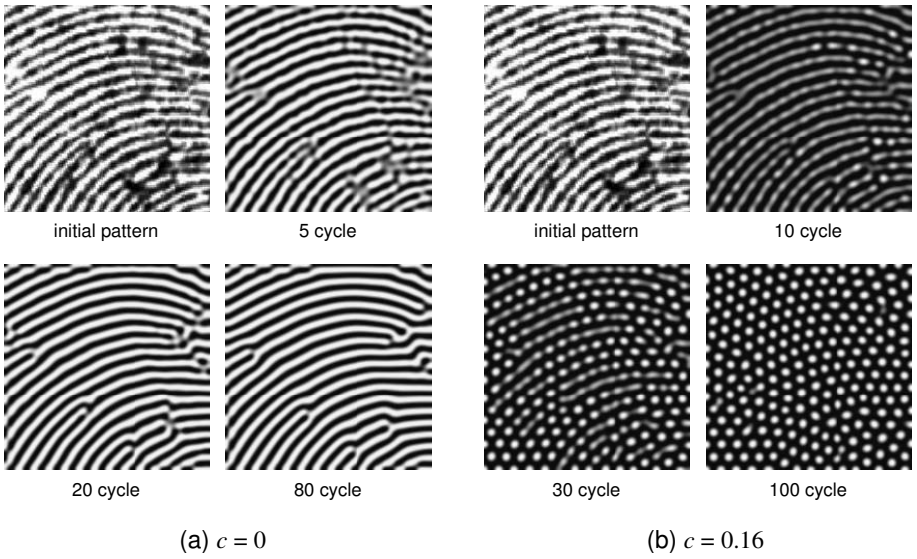

Fig. 8. Snapshots of pattern formation from initial fingerprint image.

100 cycles (16,000 clocks) until it reached equilibrium to restore the spotted patterns.

The number of cycles for generating equilibrium patterns only depends on the width of the stripes (radius of spots), and is independent of image size. This implies that the power consumed by repeating these calculations is significantly reduced when the number of pixels increases. Buffers and differential amplifiers can be turned off during static periods in the system clock to reduce static power consumption in a cell. These properties enabled us to develop a low-power LSI to restore striped and spotted patterns.

5 Summary

We proposed a novel RD model that is suitable for LSI implementation and its basic LSI architecture. We developed image-processing LSI circuits based on pattern formation in reaction-diffusion (RD) systems. We introduced continuous diffusion fields and an analog state variable to Young's local activator-inhibitor model [4]. We produced a model pattern diagram on a 2D parameter space through extensive numerical simulations. We showed that the spatial frequency and form (striped or spotted) could be controlled with only two parameters. We then designed a basic circuit for the proposed model. We designed an RD LSI based on the analog computing method where the concentration of chemicals was represented by a 2D voltage distribution and the cell voltage was diffused step by step. By mimicking two diffusion fields with the proposed model in one diffusion circuit on the LSI, we reduced the area of the unit cell circuit. We confirmed the

operations of the LSI were as expected through circuit simulations. Finally, we demonstrated fingerprint image restoration on the LSI and that it successfully restored smooth striped and spotted images from noisy input images.

Acknowledgment

This study was partly supported by Industrial Technology Research Grant Program in '04 from New Energy and Industrial Technology Development Organization (NEDO) of Japan, and a Grant-in-Aid for Young Scientists [(B)17760269] from the Ministry of Education, Culture Sports, Science and Technology (MEXT) of Japan.

References

1. Turing, A.M. The chemical basis of morphogenesis. Phil. Trans. R. Soc. Lond. **B 237** (1952) 37–72.
2. Nicolis, G. & Prigogine, I.: Self-organization in Nonequilibrium Systems — From Dissipative Structures to Order through Fluctuations. John Wiley & Sons, Inc., New York (1977).
3. Murray, J.D.: Mathematical Biology I & II (3rd Ed.). Springer, New York (2002).
4. Young, D.A. A local activator-inhibitor model of vertebrate skin patterns. Math. Biosci. **72** (1984) 51–58.
5. Gerhardt M. & Schuster H., A cellular automaton describing the formation of spatially ordered structures in chemical systems. Physica D. **36** (1989) 209–221.
6. Gerhardt M., Schuster H. & Tyson J. J., A cellular automaton model of excitable media II. Curvature, dispersion, rotating waves and meandering waves. Physica D **46** (1990) 392–415.,
7. Markus M. & Hess B., Isotropic cellular automaton for modeling excitable media. Nature, **347** (1990) 56–58,
8. Weimar J. R., Tyson J. J., & Watson L. T., Diffusion and Wave Propagation in Cellular Automata Models for Excitable Media. Physica D **55** (1992) 309–327,
9. Weimar J. R. & Boon J.-P., Class of Cellular Automata for Reaction-Diffusion Systems. Phys. Rev. E **49** (1994) 1749–1752.
10. Schepers H. & Markus M., Two types of performance of aniIsotropic cellular automaton: stationary (Turing) patterns and spiral waves. Physica A **188** (1992) 337–343,
11. Kusch I. & Markus M., Mollusc shell pigmentation: cellular automaton simulations and evidence for undecidability. J. Theor. Biol. 178, 333-340 (1996).